POLITECNICO DI TORINO
Repository ISTITUZIONALE

Ethanol breath measuring system

(Article begins on next page)

20 September 2024

Ethanol breath measuring system

Luca Lombardo
Dept. of Electronics and Telecommunications
Politecnico di Torino
Torino, Italy
luca.lombardo@polito.it

Sabrina Grassini
Dept. of Applied Science and Technology
Politecnico di Torino
Torino, Italy
sabrina.grassini@polito.it

Marco Parvis
Dept. of Electronics and Telecommunications
Politecnico di Torino
Torino, Italy
marco.parvis@polito.it

Nicola Donato
Dept. of Engineering
University of Messina
Messina, Italy
nicola.donato@unime.it

Alessio Gullino
Dept. of Electronics and Telecommunications
Politecnico di Torino
Torino, Italy
alessio.gullino@polito.it

Abstract—**Driving after drinking is considered extremely dangerous and severe limits to alcohol drink before driving are enforced in several countries. This paper describes a simple and cheap device which is capable of estimating the blood ethanol level from the expired breath. The device employs a 3 mm×6 mm gas sensor based on Nb_2O_5 thin-film which features good sensing performance towards ethanol. A suitable electronic circuit is employed in order to measure the conductivity of the gas sensor and to control its working temperature. The circuit is based on a small microcontroller board (Teensy 3.2) and some additional analog circuitry. Similar devices are already available off-the-shelf, however, most of them do not guarantee an accuracy suitable for a quantitative measurement of breath ethanol. The proposed system, instead, has been developed trying to optimize accuracy, power consumption and size. Furthermore, such a system employs a novel gas sensor based on a Nb_2O_5 sensing film, which has not yet been employed in such a field. The system allows one to set the working temperature of the sensor at its optimal value ($350\ ^\circ$C) and to simultaneously measure the sensor resistance in the range between 10 MΩ and approximately 1 GΩ. The quite low power consumption together with the very small size of the system make it very suitable for portable applications such as alcohol drive tests which can warn drivers before starting driving.**

Index Terms—**alcohol level, alcohol meters, BAC**

I. Introduction

Sensors find application in several important fields such as environmental monitoring [1], [2], industry [3] and health care [4], [5]. However, nowadays, there are many other emerging applications where the demand of sensors and related measurement systems is constantly growing up. One of these is the alcohol driving test. Driving under the influence of alcohol may be extremely dangerous as the reaction time increases also for quite limited amounts of alcohol. Most countries have specific limits for the Blood Alcohol Content (BAC) for driving, which generally is 0.5 g/l, decreasing to 0 g/l for newly licensed drivers. The police usually employ non-invasive breath measuring detectors to check the amount of alcohol in the blood stream obtaining the so called breath analyzer able to measure the Breath Alcohol Content (BrAC)

which is usually converted to the BAC by means of a conventional equation. As an example, Table I shows the BAC allowed to drive in some countries.

TABLE I
ALLOWED BAC LEVEL

Country	Experienced drivers	Not experienced drivers
USA	0.05% - 0.08%	0% - 0.02%
Canada	0.08%	0
Germany	0.05%	0
Italy	0.05%	0

Of course BrAC is not an exact representation of the amount of blood alcohol content [6] and, in addition, the BrAC changes according to time, fasting condition, and so on. However, it is a simple and easy way to quickly test drivers. In some countries, the driver, which knows his/her BAC may be misleading can ask to be taken to an hospital to have a blood sample to be taken and analyzed.

Several devices have been introduced to sense the alcohol in breath [7]–[10] which may require some form of pre-heating and which can work at room temperature [12]. These devices can read the alcohol content after 10 s $- 15$ s of their turn on, have a very low cost and have a dimension which usually is of several tens of cubic centimeters. Some sensing platforms have been developed to monitor in real-time several parameters in the field of remote healthcare [13], [14], however they typically feature larger dimensions, require a Internet connection and are not suitable for portable applications.

The device here described belongs to the heated sensor arena, so it requires some seconds before being ready. Such device is similar to the already available, with the exception of being with a volume of few cubic centimeters so being really small and easy to carry out. Moreover, it is completely self-sufficient and does not require any support device or Internet connection.

Converting the BrAC to BAC is a complex and questionable operation which involves the 'normal' ethanol transfer from

blood to breath. However, the following simple equation, herein used for clarity, is able to satisfactorily estimate the BAC from the BrAC:

$$BAC = \frac{BrAC}{2600} \qquad (1)$$

where the $BrAC$ is expressed in part per million (ppm), and the BAC is expressed in % to be compliant to the different country regulations.

This means that, with all the limitations expressed above, a BAC of 0.05% is equivalent to a concentration in the breath of the order of 130 ppm.

II. The proposed alcohol measuring system

A suitable measuring system was developed in order to interface the ethanol gas sensor and to estimate the BAC levels from measurements of the ethanol breath concentration (BrAC). The block diagram of such a system is shown in Fig. 1.
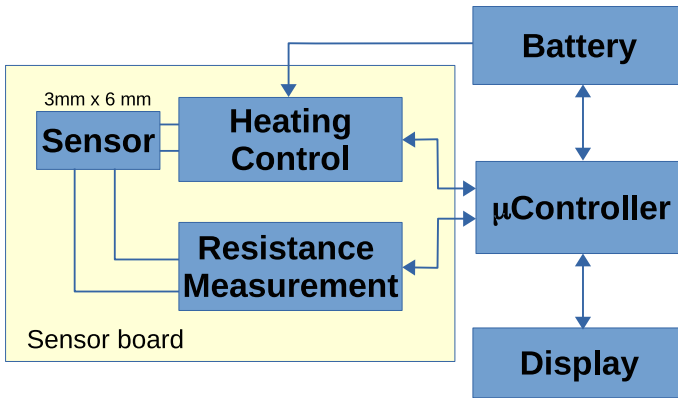

Fig. 1. The proposed measuring system able to estimate the BAC level.

The figure shows:
- A sensor board which contains:
  - the ethanol gas sensor, described later, which has the dimension of 3 mm $\times 6$ mm. The sensor features a small platinum heater on one side and a couple of inter-digitated electrodes on the other side. A thin layer of Nb_2O_5 is deposed by using a plasma reactor on the inter-digitated electrodes and it acts as the sensing layer.
  - The circuit which is used to drive the platinum heater to bring the sensor at the most suitable working temperature.
  - The circuit referred to as "Resistance Measurement", which is used for measuring the inter-digitated electrode resistance and, therefore, to estimate the BAC.
- The micro-controller, which is used to drive the heater, to read the resistance, and to drive the LCD display. In the actual implementation, the micro-controller is an off-the-shelf Teensyduino 3.2. However, any similar device can be used as well.
- The LCD display, used to visualize the measurements.

- The battery for powering the system, whose duration is mainly related to the sensor heating.

III. The sensitive element

The sensitive element is based on a small 3 mm $\times 6$ mm alumina substrate, treated in a plasma reactor to coat the sensitive part with a thin Nb_2O_5 layer [5].

In such type of sensors, known as conductometric metal-oxide gas sensors, there is a relationship between the target gas concentration and the relative change of the sensor resistance. The specific sensor prototype employed in the proposed breath analyzer was realized depositing a thin film of Nb_2O_5 by reactive plasma sputtering. The film was deposited from an high-purity niobium target (99.99%) with a RF power of 250 W for 30 min in a mixture of Ar (99.99%) and O_2 (99.99%) at flow rates of 50 sccm and 20 sccm (standard cubic centimeters per minute), respectively. The resulting Nb_2O_5 film is characterized by a quite compact structure and a thickness of about 200 nm.

The niobium penta-oxyde features good sensing performance towards ethanol (and towards acetone) as described in more details in [10], [11].

IV. The sensor board

The sensor board, in addition to the Teensyduino microcontroller, contains two main components: the heating control system and the electronic circuit to measure the sensor resistance.

The best sensing performance for such a gas sensor are obtained at a working temperature of about 350 °C. Therefore, a heating system is employed in order to accurately control the sensor temperature. The heating system circuit, shown in Fig. 2, uses the sensor platinum heater both as heating element and temperature probe taking advantage by its temperature coefficient.
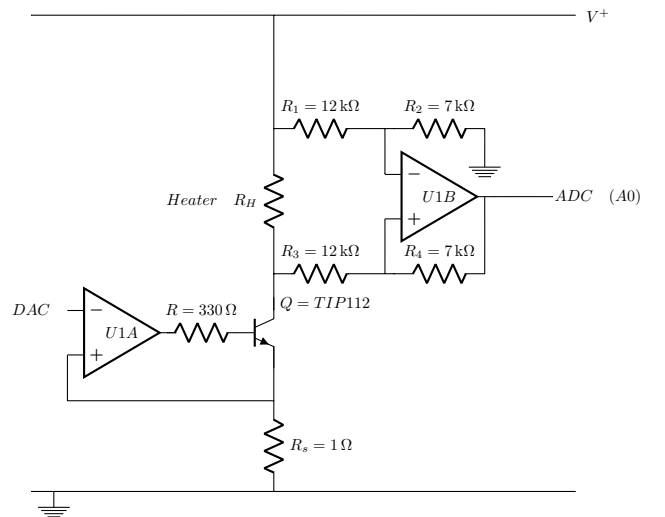

Fig. 2. Electronic circuit of the heating system.

The system employs the micro-controller Digital-to-Analog Converter (DAC) output to set a suitable heater current by means of the operational amplifier A1A, the current-boost bipolar transistor Q and the current-sense resistor R_s. At the same time, the voltage drop across the heater (R_H) is measured by the operational amplifier A1B, mounted in a differential amplifier configuration, and the analog channel A0 of the micro-controller Analog-to-Digital Converter (ADC).

In such a way, the micro-controller is able to measure the heater resistance and, therefore, the sensor temperature. A software-implemented closed-loop temperature controller based on a hysteresis approach is employed to stabilize the sensor working temperature at about 350 °C with an accuracy of about 10 °C. The control system is designed to switch off the heater current with a frequency of about 0.1 s therefore leaving the substrate at a nearly constant temperature and, at the same time, reducing the power consumption.
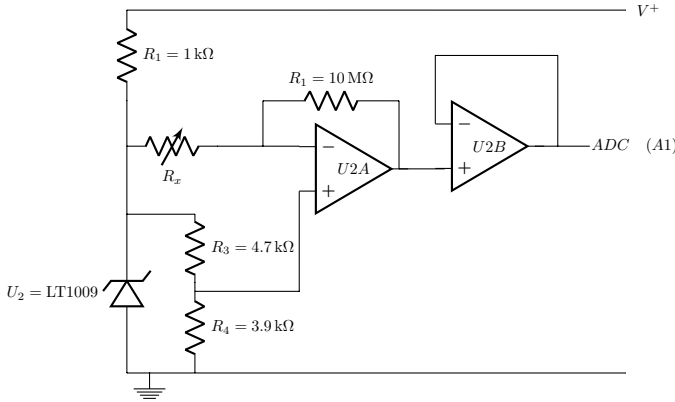

Fig. 3. Electronic circuit of the resistance measurement system.

The resistance measurement circuit is shown in Fig. 3 and is composed by two operational amplifiers. The sensor resistance is measured by forcing a known constant voltage across the sensor and measuring the current flowing throughout the sensor itself. This is accomplished by the first operational amplifier (U2A) which works as transimpedance circuit with a feedback resistance of 10 MΩ. Since the sensor resistance is expected to change in the range between 20 MΩ and about 1 GΩ, the current is expected to be of the order of few nanoamperes and this requires the use of low-bias operational amplifiers. The sensor measurement voltage ΔV is fixed at about 1.14 V by means of the voltage reference U_2 ($V_{ref} = 2.5V$) and a voltage divider (R_3 and R_4). A second operational amplifier (U2B) is used simply as voltage buffer in order to uncouple the transimpedance amplifier from the micro-controller digital noise. The output voltage is subsequently measured by the analog channel A1 of the micro-controller ADC which features a resolution of 16-bit.

The output voltage of the circuit is inversely proportional to the sensor resistance R_x, as resulting from the input-output relationship:

$$V_{out} = V_{bias} - \frac{R_1}{R_x}\Delta V \qquad (2)$$

where V_{bias} is the voltage at the non-inverting input of U2A and R_x is the sensor resistance. As consequence, the output voltage saturates at the V_{bias} voltage for resistances higher than approximately 2 GΩ and at the ground rail for resistances lower than about 10 MΩ.

The bias and stray currents of the first operational amplifier are of the order of tens of pA while the voltage offset is of the order of few millivolts. Such components, even though quite small, become significant for resistance in the order of 1 GΩ and cannot be considered negligible. Therefore, a calibration procedure was implemented in the micro-controller firmware in order to compensate for the effects of both offset and parasitic currents.

V. EXPERIMENTAL RESULTS

Preliminary characterizations of the measuring system were carried out separately for the heating system and the resistance measuring circuit in order to evaluate their performance and accuracy.

A. Heater system characterization

Initially the sensor has been characterized to see if the heating system is capable of changing the sensor temperature and keep it at a fixed value with a suitable accuracy.
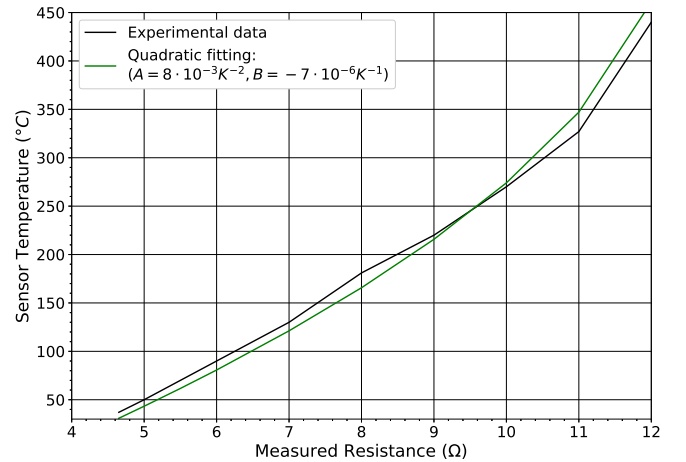

Fig. 4. Results of the test performed on the sensor heater.

To this aim a thermocouple was put in contact with the sensing area of the gas sensor while the software on the Teensyduino was requested to keep the heater resistance at a fixed values in the range between about 4 Ω and 12 Ω. The sensor temperature was, therefore, measured with the thermocouple at several different resistance values. Results of this test are shown in Fig. 4. The black line reports the temperature as measured by the thermocouple versus the resistance requested to the heater and obtained by the scaled measurement performed by the micro-controller ADC (channel A0). The thermocouple uncertainty is of the order

of 2 °C while the resistance is controlled by the software within 0.05 Ω, which correspond to a temperature change of about 5 °C at the maximum temperature value. Such a value cannot be considered the uncertainty on the temperature value, since different sensors can have different resistance values at room temperature. One should also note that the relation between heater resistance and temperature is different from a pure PT material for which the Calendar-Van Dusen equation hold due to the platinum purity and the porous microstructure. In fact, the A coefficient [11] is, in this case, of the order of $8 \cdot 10^{-3}$ °C^{-1} instead of the canonical Calendar-Van Dusen value of about $3.9 \cdot 10^{-3}$ °C^{-1}. The green line in Fig. 2 shows the temperature approximation obtained by using a second order polynomial equation like in the Calendar-Van Dusen formula.

B. Heater system startup time and power consumption

As explained before, the sensor needs to be heated at about 350 °C to reach the required sensitivity and this requires a warm-up time and some power which is provided by the batteries supplying the system.
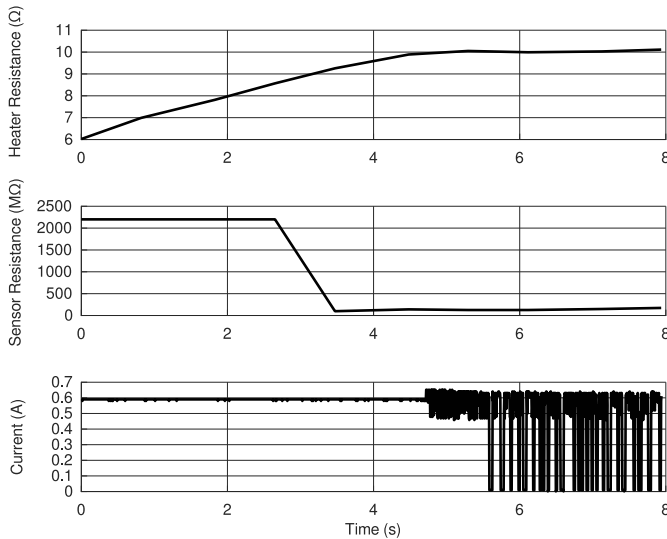
Fig. 5. Results of the test performed on the heater to determine the heating transient.

In order to check the power requirement a test was carried out with all system working and measuring the sensor resistance. Fig. 5 shows an example of such transient with the heating resistance, from which the temperature can be estimated by using the results of Fig. 2, the sensor resistance and the current required from the battery.

The figure shows how the warm-up transient lasts less than 5 s during which the current is of the order of 0.6 A. Later, the software keep the heater resistance fixed starting chopping the current in it so that the average current requirement decreases.

The measured resistance is quite high in the initial phase and the system saturates to about 2 GΩ. As the heater resistance

increases the measured resistance decreases to a value which is connected to the amount of ethanol in the breath.
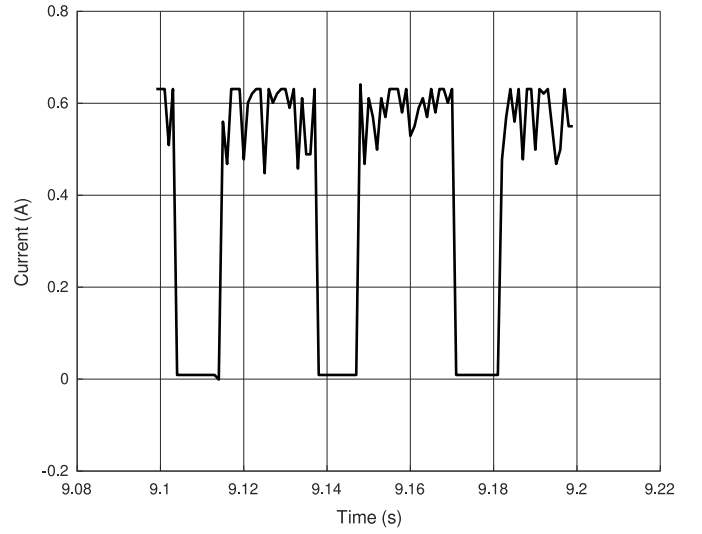
Fig. 6. Expanded results of the test performed on the heater to determine the heating transient.

Fig. 6 shows the chopping period in an expanded scale when the heating transient is complete (i.e. after about 9 s). The chopping happens every about 130 ms with a duty cycle of about 62%. In such conditions, the heater resistance is about 10 Ω which corresponds to a temperature of about 300 °C.

The power current requirement is, therefore, of about 0.6 A for the first 5 s and of about 0.4 A for the remaining measurement time. Considering a measurement time of the order of 10 s plus the heating time, a requirement of about 2 mAh for each measurement is required by the system. If the system is powered by standard AA batteries with a capacity of the order of 2400 mAh this results in a battery life of about 1200 measurements. If AAA batteries with a capacity of 1000 mAh are used, a battery life of about 500 measurements is instead obtained. In both cases, a quite long battery life is achieved thanks to the small size of the sensor and the heating control approach.

C. Characterization of the resistance measurement circuit

A dedicated test was carried out in order to characterize the performance and the accuracy of the resistance measurement system. With this aim, a bunch of precision resistors in the range between 10 MΩ and 1.3 GΩ were measured both with the proposed system and a certified bench multimeter (Agilent 34411A).

Fig. 7 shows the output voltage of the resistance measurement circuit as measured with the micro-controller ADC at the analog channel A1 (blue line) and the expected input-output characteristic of the circuit (black dashed line). It is possible to see the almost perfect agreement between the theoretical characteristic and the experimental measurements.
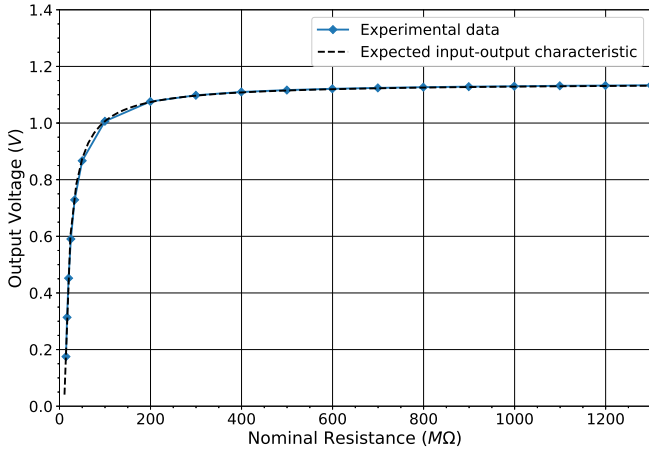
Fig. 7. Output voltage of the resistance measurement system.

The relative error due to the proposed measurement system was subsequently evaluated by comparing the measured resistor values and the expected values, as measured by the bench multimeter. The data, shown in Fig. 8, highlight a relative error lower than 1% over all the tested range between $10\ \mathrm{M\Omega}$ and $1.3\ \mathrm{G\Omega}$. Such a result is quite good if one consider the simplicity of the measurement circuit, the wide measurement range (covering more than two decades) and the accuracy achieved by bench meters which, in such a range, is typically in the order of some percent point.
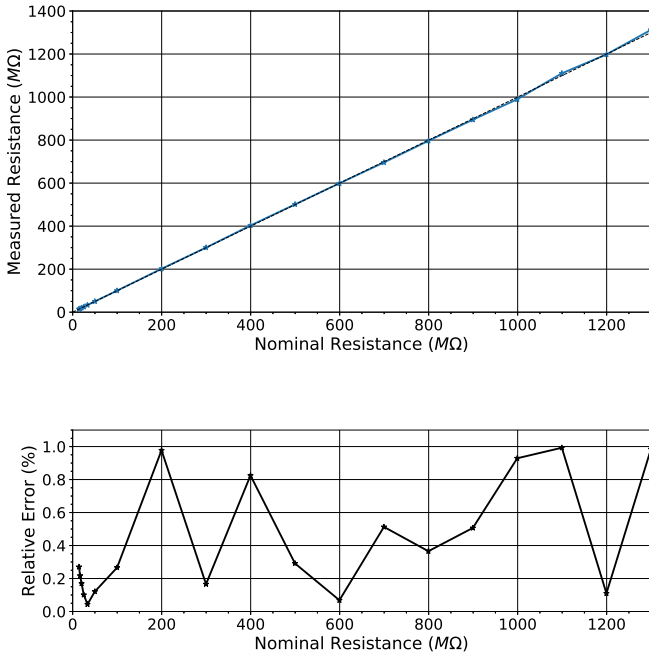

Fig. 8. Accuracy of the proposed system and relative error over the tested resistance range.

D. Ethanol measurements

Measuring the ethanol content in the expired breath is difficult due to the lack of a measuring standard. One could use a calibrated instrument, but usually such devices have a large uncertainty which prevents them to be used as a reference. The authors, therefore, decided to characterize the measurement system employing the standard flow-through approach which allows one accurately to assess the sensing performance of gas sensors.

The gas sensor prototype was connected to the proposed measuring system and placed inside a small measurement chamber. A set of mass flow meters connected to certified gas bottles was arranged in order to achieve an accurate mixture of ethanol in dry synthetic air (20% O_2, 80% N_2). The ethanol concentration was changed in the range between $10\ \mathrm{ppm}$ to $400\ \mathrm{ppm}$ while measuring the gas sensor resistance. The sensor working temperature was maintained constant at $350\ ^\circ\mathrm{C}$ during the whole test. Fig. 9 shows the acquired data. In particular, the sensor resistance is about $700\ \mathrm{M\Omega}$ in pure air and progressively decreases down to about $30\ \mathrm{M\Omega}$ when ethanol concentration increases. The same data highlight how the sensor response is almost perfectly reversible with a resistance returning to its reference value after ethanol is removed from the sampling gas.
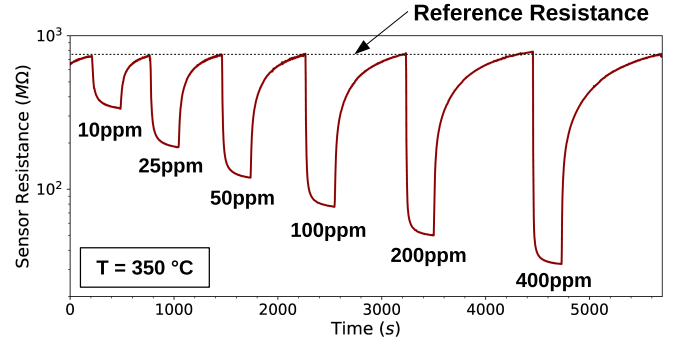

Fig. 9. Sensor relative response towards ethanol at a working temperature of $350\ ^\circ\mathrm{C}$.

An empirical calibration curve was estimated from the experimental data, as shown in Fig. 10 and embedded in the micro-controller firmware so that from a direct measurement of the sensor resistance it is possible to calculate the ethanol concentration (BrAC) and, from it, to estimate the blood alcohol content (BAC). The calibration curve shows how the sensor response is quite high and does not exhibit any significant saturation in the whole range typically required for BrAC measurements.

VI. CONCLUSIONS

Breath alcohol test is a valid and non-invasive method for estimate the blood alcohol content (BAC) of drivers. Nowadays, such approach is commonly employed by the police to identify drunk-driving conditions and several portable devices are available off-the-shelf at a quite low cost. Unfortunately,
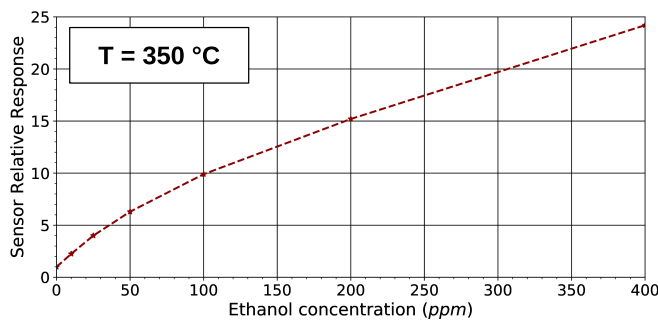
Fig. 10. Calibration curve of the proposed ethanol sensor at a working temperature of 350 °C.

most of them lack of accuracy and this represents a severe limitation in its employment.

The proposed measurement system features very small size and a quite low power consumption which allows one to perform hundreds measurement with a single battery charge. The system employs a small conductometric gas sensor based on a Nb_2O_5 thin-film deposited on an alumina substrate by reactive plasma sputtering.

Several characterization were carried out to evaluate the system performance in term of sensor heating capability, power consumption and accuracy of the sensor resistance measurement. The heating system is able to stabilize the sensor working temperature at its optimal value (about 350 °C) with an accuracy of about 10 °C. The resistance measurement system is capable to cover more than two decades in the range between about 10 MΩ to approximately 2 GΩ with a relative error lower than 1% on all over the tested range. A calibration of the system was carried out and it revealed a quite wide detection range of ethanol ranging from few ppm to more than 400 ppm. Such a range is compatible with the BrAC levels commonly found in human exhaled breath.

Therefore, from the preliminary results carried out on the sensor prototype, the measurement system revealed suitable performance to be employed in the detection of ethanol in the exhaled breath. Such performance, together with the small size and the low power consumption, make the proposed device a promising solution for low-cost portable ethanol detection.

REFERENCES

[1] L. Lombardo, M. Parvis, E. Angelini, S. Grassini, An optical sampling system for distributed atmospheric particulate matter, IEEE Transactions on Instrumentation and Measurements, Vol. 68, N. 7, pp. 2396-2403, 2019, doi: 10.1109/TIM.2019.2890885.
[2] G. Andria, G. Cavone, A. M. L. Lanzolla, Modelling study for assessment and forecasting variationin urban air pollution, Measurement, Vol. 41, N. 3, pp. 222-229, 2008.
[3] G. Andria, F. Attivissimo, A. Di Nisio, A. Trotta, S. M. Camporeale, P. Pappalardi, Design of a microwave sensor for measurement of water in fuel contamination, Measurement, Vol. 136, pp. 74-81, 2019.
[4] L. Lombardo, N. Donato, S. Grassini, A. Gullino, K. Moulaee, G. Neri, M. Parvis, High sensitive and selective mini-sensor for acetone monitoring, IEEE Transactions on Instrumentation and Measurements, doi: 10.1109/TIM.2020.2967161 (early access).
[5] L. Lombardo, Development and characterization of sensors for human health, Ph.D. Thesis in Metrology, 2019, Politecnico di Torino, Torino, Italy.
[6] L. F. Giraldo, K. M. Passino, J. D. Clapp, D. Ruderman, Dynamics of Metabolism and Decision Making During Alcohol Consumption: Modeling and Analysis, IEEE Tr. on Cybernetics, vol. 47, no. 11, pp. 3955-3966, 2017
[7] F. Alam, A. H. Jalal, N. Pala, Selective Detection of Alcohol Through Ethyl-Glucuronide Immunosensor Based on 2D Zinc Oxide Nanostructures, IEEE Sensor Journal, vol. 19, no. 11, pp. 3984-3992, 2019
[8] M. L. Y. Sin et al., Ultra-Low-Power Alcohol Vapor Sensors Based on Multi- Walled Carbon Nanotube, Proc. of the 1st IEEE Int. Con. on Nano/Micro Engineered and Molecular Systems, pp. 1198-1202, January 18 - 21, 2006, Zhuhai, China
[9] N. Banerjee, S. Roy, Alcohol sensing performance of ZnO nano-flower based resistive sensor: Comparative study, 2018 Emerging Trends in Electronic Devices and Computational Techniques (EDCT)
[10] A. Gullino, et. al, Employment of Nb2O5 thin-films for ethanol sensing, I2MTC 2020, Dubrownik, Croatia, May 25-28, 2020
[11] L. Lombardo , et. al, High sensitive and selective mini-sensor for acetone monitoring", IEEE Transactions on Intrumentation and Measurement, 10.1109/TIM.2020.2967161
[12] R. Jaisutti, K. Eaiprasertsak, T. Osotchan, Room temperature alcohol sensors based on PANi/MWCNT composite thin film, IEEE Conf. on Sensors, 2015
[13] A. Darwish, A. E. Hassanien, M. Elhoseny, et al., The impact of the hybrid platform of internet of things and cloud computing on health-care systems: opportunities, challenges, and open problems, Journal of Ambient Intelligence and Humanized Computing, 10, 4151-4166, 2019, 10.1007/s12652-017-0659-1.
[14] A. Galiano et al., Improvements in heamatology for home health assistance and monitoring by a web based communication system, 2016 IEEE International Symposium on Medical Measurements and Applications (MeMeA), Benevento, 2016, pp. 1-5.
[15] C. Antoine, Tensions des vapeurs; nouvelle relation entre les tensions et les tempè, Comptes Rendus des Séances de l'Académie des Sciences, 107: 1888.
[16] Antoine coefficients freely available at http://ddbonline.ddbst.com/AntoineCalculation/AntoineCalculationCGI.exe, last checked 2019-01-20.
[17] F.-M. Raoult, Loi gnrale des tensions de vapeur des dissolvants (General law of vapor pressures of solvents), Comptes rendus, 104 : 14301433, 1886